22. Favetta LA, Robert C, King WA, Betts DH (2004) Expression profiles of p53 and p66shc during oxidative stress-induced senescence in fetal bovine fibroblasts. Exp Cell Res 299: 36–48.
23. Hussain SP, Harris CC (2007) Inflammation and cancer: an ancient link with novel potentials. Int J Cancer 121: 2373–2380.
24. Stewart B, Kleihues P (2003) The Causes of Cancer. In: World Cancer Report. Lyon: IARC Press. 56–61.
25. Prueitt RL, Boersma BJ, Howe TM, Goodman JE, Thomas DD, et al. (2007) Inflammation and IGF-I activate the Akt pathway in breast cancer. Int J Cancer 120: 796–805.
26. Mantovani A, Schioppa T, Porta C, Allavena P, Sica A (2006) Role of tumor-associated macrophages in tumor progression and invasion. Cancer Metastasis Rev 25: 315–322.
27. Pollard JW (2009) Trophic macrophages in development and disease. Nat Rev Immunol 9: 259–270.
28. Thomas DD, Ridnour LA, Isenberg JS, Flores-Santana W, Switzer CH, et al. (2008) The chemical biology of nitric oxide: implications in cellular signaling. Free Radic Biol Med 45: 18–31. S0891–5849(08)00175–5 [pii];10.1016/j.freeradbiomed.2008.03.020 [doi].
29. Thomas DD, Espey MG, Ridnour LA, Hofseth LJ, Mancardi D, et al. (2004) Hypoxic inducible factor 1alpha, extracellular signal-regulated kinase, and p53 are regulated by distinct threshold concentrations of nitric oxide. Proc Natl Acad Sci U S A 101: 8894–8899.
30. Campisi J, Andersen JK, Kapahi P, Melov S (2011) Cellular senescence: A link between cancer and age-related degenerative disease? Semin Cancer Biol. S1044–579X(11)00050–2 [pii];10.1016/j.semcancer.2011.09.001 [doi].
31. Boersma BJ, Howe TM, Goodman JE, Yfantis HG, Lee DH, et al. (2006) Association of breast cancer outcome with status of p53 and MDM2 SNP309. J Natl Cancer Inst 98: 911–919.
32. Cox GW, Mathieson BJ, Gandino L, Blasi E, Radzioch D, et al. (1989) *Heterogeneity of hematopoietic cells immortalized by v-myc/v-raf recombinant* retrovirus infection of bone marrow or fetal liver. J Natl Cancer Inst 81: 1492–1496.
33. Dimri GP, Lee X, Basile G, Acosta M, Scott G, et al. (1995) A biomarker that identifies senescent human cells in culture and in aging skin in vivo. Proc Natl Acad Sci U S A 92: 9363–9367.
34. Kumamoto K, Spillare EA, Fujita K, Horikawa I, Yamashita T, et al. (2008) Nutlin-3a activates p53 to both down-regulate inhibitor of growth 2 and up-regulate mir-34a, mir-34b, and mir-34c expression, and induce senescence. Cancer Res 68: 3193–3203.
35. Espey MG, Miranda KM, Pluta RM, Wink DA (2000) Nitrosative capacity of macrophages is dependent on nitric-oxide synthase induction signals. J Biol Chem 275: 11341–11347.
36. Ridnour LA, Windhausen AN, Isenberg JS, Yeung N, Thomas DD, et al. (2007) Nitric oxide regulates matrix metalloproteinase-9 activity by guanylyl-cyclase-dependent and -independent pathways. Proc Natl Acad Sci U S A 104: 16898–16903. 0702761104 [pii];10.1073/pnas.0702761104 [doi].
37. Lundberg JO, Hellstrom PM, Lundberg JM, Alving K (1994) Greatly increased luminal nitric oxide in ulcerative colitis. Lancet 344: 1673–1674.
38. Kuilman T, Michaloglou C, Vredeveld LC, Douma S, van Doorn R, et al. (2008) Oncogene-induced senescence relayed by an interleukin-dependent inflammatory network. Cell 133: 1019–1031.
39. Fujita K, Mondal AM, Horikawa I, Nguyen GH, Kumamoto K, et al. (2009) p53 isoforms Delta133p53 and p53beta are endogenous regulators of replicative cellular senescence. Nat Cell Biol 11: 1135–1142.
40. Schetter AJ, Leung SY, Sohn JJ, Zanetti KA, Bowman ED, et al. (2008) MicroRNA expression profiles associated with prognosis and therapeutic outcome in colon adenocarcinoma. JAMA 299: 425–436.
41. Schetter AJ, Nguyen GH, Bowman ED, Mathe EA, Yuen ST, et al. (2009) Association of inflammation-related and microRNA gene expression with cancer-specific mortality of colon adenocarcinoma. Clin Cancer Res 15: 5878–5887.
42. DePinho RA (2000) The age of cancer. Nature 408: 248–254.
43. O'Sullivan JN, Bronner MP, Brentnall TA, Finley JC, Shen WT, et al. (2002) Chromosomal instability in ulcerative colitis is related to telomere shortening. Nat Genet 32: 280–284.
44. Risques RA, Lai LA, Himmetoglu C, Ebaee A, Li L, et al. (2011) Ulcerative colitis-associated colorectal cancer arises in a field of short telomeres, senescence, and inflammation. Cancer Res 71: 1669–1679. 0008–5472.CAN-10-1966 [pii];10.1158/0008–5472.CAN-10-1966 [doi].
45. Campisi J, Andersen JK, Kapahi P, Melov S (2011) Cellular senescence: A link between cancer and age-related degenerative disease? Semin Cancer Biol. S1044–579X(11)00050–2 [pii];10.1016/j.semcancer.2011.09.001 [doi].
46. Rogakou EP, Pilch DR, Orr AH, Ivanova VS, Bonner WM (1998) DNA double-stranded breaks induce histone H2AX phosphorylation on serine 139. J Biol Chem 273: 5858–5868.
47. Jackson SP, Bartek J (2009) The DNA-damage response in human biology and disease. Nature 461: 1071–1078.
48. Coppe JP, Patil CK, Rodier F, Sun Y, Munoz DP, et al. (2008) Senescence-associated secretory phenotypes reveal cell-nonautonomous functions of oncogenic RAS and the p53 tumor suppressor. PLoS Biol 6: 2853–2868.
49. Connelly L, Jacobs AT, Palacios-Callender M, Moncada S, Hobbs AJ (2003) Macrophage endothelial nitric-oxide synthase autoregulates cellular activation and pro-inflammatory protein expression. J Biol Chem 278: 26480–26487.
50. Thomas DD, Ridnour LA, Espey MG, Donzelli S, Ambs S, et al. (2006) Superoxide fluxes limit nitric oxide-induced signaling. J Biol Chem 281: 25984–25993.
51. Clemons NJ, McColl KE, Fitzgerald RC (2007) Nitric oxide and acid induce double-strand DNA breaks in Barrett's esophagus carcinogenesis via distinct mechanisms. Gastroenterology 133: 1198–1209.
52. Dickey JS, Baird BJ, Redon CE, Sokolov MV, Sedelnikova OA, et al. (2009) Intercellular communication of cellular stress monitored by gamma-H2AX induction. Carcinogenesis 30: 1686–1695. bgp192 [pii];10.1093/carcin/bgp192 [doi].
53. Forrester K, Ambs S, Lupold SE, Kapust RB, Spillare EA, et al. (1996) Nitric oxide-induced p53 accumulation and regulation of inducible nitric oxide synthase expression by wild-type p53. Proc Natl Acad Sci U S A 93: 2442–2447.
54. Ambs S, Merriam WG, Ogunfusika MO, Bennett WP, Ishibe N, et al. (1998) p53 and vascular endothelial growth factor regulate tumor growth of NOS2-expressing human carcinoma cells. Nat Med 4: 1371–1376.
55. Bhaumik D, Scott GK, Schokrpur S, Patil CK, Orjalo AV, et al. (2009) MicroRNAs miR-146a/b negatively modulate the senescence-associated inflammatory mediators IL-6 and IL-8. Aging (Albany NY) 1: 402–411.
56. Wu F, Zikusoka M, Trindade A, Dassopoulos T, Harris ML, et al. (2008) MicroRNAs are differentially expressed in ulcerative colitis and alter expression of macrophage inflammatory peptide-2 alpha. Gastroenterology 135: 1624–1635.
57. Simone NL, Soule BP, Ly D, Saleh AD, Savage JE, et al. (2009) Ionizing radiation-induced oxidative stress alters miRNA expression. PLoS One 4: e6377.
58. Mathe E, Nguyen GH, Funamizu N, He P, Moake M, et al. (2011) Inflammation regulates microRNA expression in cooperation with p53 and nitric oxide. Int J Cancer. 10.1002/ijc.26403 [doi].
59. Weber M, Baker MB, Moore JP, Searles CD (2010) MiR-21 is induced in endothelial cells by shear stress and modulates apoptosis and eNOS activity. Biochem Biophys Res Commun 393: 643–648. S0006–291X(10)00256–1 [pii];10.1016/j.bbrc.2010.02.045 [doi].
60. Shin VY, Jin H, Ng EK, Cheng AS, Chong WW, et al. (2011) NF-kappaB targets miR-16 and miR-21 in gastric cancer: involvement of prostaglandin E receptors. Carcinogenesis 32: 240–245. bgq240 [pii];10.1093/carcin/bgq240 [doi].
61. DeNicola GM, Tuveson DA (2009) RAS in cellular transformation and senescence. Eur J Cancer 45 Suppl 1: 211–216. S0959–8049(09)70036-X [pii];10.1016/S0959–8049(09)70036-X [doi].
62. Frezzetti D, Menna MD, Zoppoli P, Guerra C, Ferraro A, et al. (2011) Upregulation of miR-21 by Ras in vivo and its role in tumor growth. Oncogene 30: 275–286. onc2010416 [pii];10.1038/onc.2010.416 [doi].
63. Oliveira CJ, Schindler F, Ventura AM, Morais MS, Arai RJ, et al. (2003) Nitric oxide and cGMP activate the Ras-MAP kinase pathway-stimulating protein tyrosine phosphorylation in rabbit aortic endothelial cells. Free Radic Biol Med 35: 381–396. S0891584903003113 [pii].
64. Abraham C, Cho JH (2009) Inflammatory bowel disease. N Engl J Med 361: 2066–2078.
65. McGovern DP, Gardet A, Torkvist L, Goyette P, Essers J, et al. (2010) Genome-wide association identifies multiple ulcerative colitis susceptibility loci. Nat Genet 42: 332–337.
66. Franke A, McGovern DP, Barrett JC, Wang K, Radford-Smith GL, et al. (2010) Genome-wide meta-analysis increases to 71 the number of confirmed Crohn's disease susceptibility loci. Nat Genet 42: 1118–1125. ng.717 [pii];10.1038/ng.717 [doi].
67. Rivas MA, Beaudoin M, Gardet A, Stevens C, Sharma Y, et al. (2011) Deep resequencing of GWAS loci identifies independent rare variants associated with inflammatory bowel disease. Nat Genet 43: 1066–1073. ng.952 [pii];10.1038/ng.952 [doi].
68. Hedl M, Li J, Cho JH, Abraham C (2007) Chronic stimulation of Nod2 mediates tolerance to bacterial products. Proc Natl Acad Sci U S A 104: 19440–19445.
69. Maeda S, Hsu LC, Liu H, Bankston LA, Iimura M, et al. (2005) Nod2 mutation in Crohn's disease potentiates NF-kappaB activity and IL-1beta processing. Science 307: 734–738.
70. Baker DJ, Wijshake T, Tchkonia T, LeBrasseur NK, Childs BG, et al. (2011) Clearance of p16Ink4a-positive senescent cells delays ageing-associated disorders. Nature 479: 232–236. nature10600 [pii];10.1038/nature10600 [doi].

International Immunology, Vol. 24, No. 1, pp. 17–27
doi:10.1093/intimm/dxr089
Advance Access publication 20 December 2011

B cells regulate antibody responses through the medullary remodeling of inflamed lymph nodes

Jun Abe[1,2], Satoshi Ueha[1,2], Hiroyuki Yoneyama[3], Yusuke Shono[1,4], Makoto Kurachi[1,2,5,6], Akiteru Goto[7], Masashi Fukayama[7], Michio Tomura[1,8], Kazuhiro Kakimi[9] and **Kouji Matsushima[1,2]**

[1]Department of Molecular Preventive Medicine, Graduate School of Medicine, The University of Tokyo, 7-3-1, Hongo, Bunkyo-ku, Tokyo 113-0033, Japan
[2]Japan Science and Technology Agency, CREST program, Tokyo 102-0076, Japan
[3]Stelic Institute & Co, Tokyo 106-0044, Japan
[4]Department of Hematology, Graduate School of Medicine, Hokkaido University, Sapporo 060-8638, Japan
[5]MD Scientist Training Program, Graduate School of Medicine, The University of Tokyo, Tokyo 113-0033, Japan
[6]Center for NanoBio Integration (CNBI), The University of Tokyo, Tokyo 113-0033, Japan
[7]Department of Pathology, Graduate School of Medicine, The University of Tokyo, 7-3-1, Hongo, Bunkyo-ku, Tokyo 113-0033, Japan
[8]Center for Innovation in Immunoregulative Technology and Therapeutics, Graduate School of Medicine, Kyoto University, Kyoto 606-8501, Japan
[9]Department of Immunotherapeutics, Graduate School of Medicine, The University of Tokyo, Tokyo 113-8655, Japan

Correspondence to: K. Matsushima; E-mail: koujim@m.u-tokyo.ac.jp

Received 10 August 2011, *accepted* 12 October 2011

Abstract

Lymph node (LN) structure is remodeled during immune responses, a process which is considered to play an important role in the regulation of immune function. To date, little attention has been paid to the remodeling of the medullary region, despite its proposed role as a niche for antibody-producing plasma cells. Here, we show that B cells mediate medullary remodeling of antigen-draining LNs during inflammation. This process occurs with kinetics similar to changes in plasma cell number and is accompanied by stromal renetworking which manifests as the segregation of B cells and plasma cells. Medullary remodeling depends on signaling via the lymphotoxin-β receptor and the presence of B cells but occurs independently of T-dependent humoral responses or other immune cell subsets including T cells, monocytes and neutrophils. Moreover, reconstitution of non-cognate polyclonal B cells in B cell-deficient mice restores not only the medullary remodeling but also the antibody response by separately transferred cognate B cells, suggesting that non-cognate B cells contribute to antibody responses through medullary remodeling. We propose that non-cognate B cells mediate the expansion of the plasma cell niche in LN through medullary remodeling, thereby regulating the size of the LN plasma cell pool.

Keywords: lymphotoxin, non-cognate B cell, plasma cell niche

Introduction

Lymph nodes (LNs) are distributed throughout the body in order to efficiently harvest antigens (1). Antigen surveillance by immune cells is a pivotal process for the induction of immune responses and tolerance. Stromal networks play a vital role in this process, providing structural support and guiding cue for immune cell accumulation, motility and interaction in LNs (2–6). Each compartment of the LN—the B-cell region (follicles), the T-cell region (paracortex) and the medulla—contains different stromal networks, which are optimized to support the events taking place within that compartment (4).

Of the three compartments of the LN, the medulla contains the least lymphocytes under naive conditions. However, the LN medulla is implicated in various aspects of immune function, including antigen uptake and clearance (7–9), lymphocyte trafficking (10,11) and the proliferation and antibody production of B cells and plasma cells (12,13). One of the most investigated features of the LN medulla is its relationship to antibody responses that play an important role in both host defense and in the development of allergic and autoimmune diseases (14,15). Most of the plasma cells generated and residing in LNs are localized to the medulla (16) and produce massive amounts of antigen-specific antibodies in order to achieve the clearance and containment of antigens. A recent report suggests that myeloid cells, and possibly stromal cells, in the LN medulla possess a unique growth factor expression profile under inflammatory conditions (17), creating a cytokine

milieu that promotes plasma cell survival. Notably, plasma cells residing in the medulla are immotile *in vivo* (16,18), despite their chemotactic ability *in vitro* (19), raising a possibility that the medullary microenvironment induces plasma cell immobility. As a result, the accumulating plasma cells are retained in the proximity of the lymphatic sinus, which enables them to direct antibody to the circulation. These observations suggest that the LN medulla functions as a plasma cell niche. Moreover, such a niche is likely to be created or expanded during immune responses because most LNs are virtually devoid of plasma cells and have little medullary parenchyma in non-inflamed conditions.

The size of antigen-draining LNs (DLNs) expands vigorously during immune responses against infection, tumors and adjuvant-based vaccination. This process is accompanied by the structural remodeling of the LNs that manifests as the re-networking and re-organization of reticular fibers and vasculature (20–26). LN remodeling facilitates the recruitment of lymphocytes and dendritic cells (DCs) and also creates a scaffold for proliferating and newly recruited T cells, B cells and DCs (21,22). Moreover, increases in stromal cell numbers during LN remodeling may also expand the availability of the lymphocyte survival factors IL-7 and B-cell activating factor (BAFF) (27,28), which are derived from stromal cells. Therefore, LN remodeling provides a structural support for the activation and differentiation of cognate lymphocytes, thereby contributing to the creation or expansion of a niche for plasma cells and other effector/memory cells.

Previous studies on LN remodeling have mostly focused on B-cell and T-cell regions or the vasculature. In contrast, little is known about the remodeling of the LN medulla, although one report alluded to the possibility of medullary remodeling by showing reticular re-networking in the LN medulla during inflammation (20). Considering the role of LN remodeling, structural changes in the medulla, together with changes in leukocyte migration, could promote the retention of B cells and plasma cells. Remodeling of the LN medulla should be therefore considered as a mechanism enabling the accumulation of plasma cells in the medulla, thereby contributing to efficient delivery of antibodies throughout the body. However, to date, both the mechanism underlying medullary remodeling and its significance to the antibody response remain to be elucidated.

In this study, we examined the changes in the LN medulla that accompany its remodeling. We identified B cells and lymphotoxin-β receptor (LTβR) as cellular and molecular components responsible for the remodeling of the LN medulla. Moreover, by using B cell-deficient mice and experiments involving the adoptive transfer of B cells, remodeling of the LN medulla was found to play a role in antigen-specific antibody responses.

Methods

Mice

C57BL/6, BALB/c and BALB/c *nu/nu* mice were purchased from Japan SLC (Shizuoka, Japan). *Ccr2*$^{-/-}$, μMT, C57BL/6.SJL (CD45.1^{+}) and NP-specific BCR-knock-in (B1-8) mice were purchased from the Jackson Laboratory (Bar Harbor, ME, USA). *Cxcr5*$^{-/-}$ mice were provided by Martin Lipp (Max-Delbrück Center for Molecular Medicine). Mice were bred and maintained in our facility and were used at 6–9 weeks of age. For the generation of bone marrow (BM) chimeras, mice were irradiated with 9.5 Gy X-ray and reconstituted with 3×10^6 donor BM cells on the next day. Chimeric mice were used for experiments at least 8 weeks after reconstitution. All animal experiments were performed in accordance with the guidelines of the Animal Care and Use Committee of the University of Tokyo.

Immunization

Mice were subcutaneously immunized in the right hind hock (29) with 50 μg (4-nitrophenol)$_{30}$-ovalbumin (NP-OVA) (Biosearch Technologies, Novato, CA, USA) emulsified in CFA (BD Biosciences, San Jose, CA, USA) or adsorbed onto Alum adjuvant (Thermo Scientific, Rockford, IL, USA), 1×10^4 pfu VV-OVA (30), 5×10^4 pfu herpes simplex virus (HSV)-1 (31) or 5×10^4 cfu *Listeria monocytogenes* (LM)-OVA (32) on day 0. In some experiments, mice received 200 μg anti-mouse CD4 (GK1.5, BioXell) on days −3 and −1 or 100 μg LTβR-Ig on days −1 and 1. Popliteal LNs were used for analyses.

Antibodies

mAbs were purchased from the following manufacturers: anti-CD3 (17A2), CD11b (M1/70), CD16/32 (93), CD38 (90), CD43 (S7), CD45.1 (A20), B220 (RA3-6B2), CD90.2 (53–2.1), CD138 (281-2), NK1.1 (PK136), Ter-119 (TER-119), IgD (11-26c.2a), IgG1a (10.9), Igκ (187.1), gp38 (8.1.1) and follicular DCs (FDC-M1) from BD Biosciences, eBioscience (San Diego, CA, USA) or BioLegend (San Diego, CA, USA) and anti-CD169 (Moma-1) from Acris Antibodies (Herford, Germany). Polyclonal anti-Lyve-1 was purchased from R&D Systems (Minneapolis, MN, USA). Alexa Fluor®-labeled secondary antibodies and streptavidin were purchased from Invitrogen (Carlsbad, CA, USA).

Microdissection and quantitative PCR analysis of the LN medulla

Ten-micrometer fresh cryosections of LN were prepared on foil slides (Matsunami Glass, Osaka, Japan). Sections were fixed in 19:1 ethanol/acetic acid for 1 min and were stained with 0.05% toluidine blue for 1 min. The medullary region in each section was identified based on the medullary sinus and was isolated from the sections by LMD7000 laser microdissection apparatus equipped with DFC310 Fx camera and ×10 objective (Leica Microsystems, Wetzlar, Germany). Fragments of the medullary region were collected in TRIzol reagent (Invitrogen) and total RNA was prepared according to the manufacturer's instructions using RNase-free equipment. RNA was reverse transcribed using a High Capacity Reverse Transcription Kit (Applied Biosystems, Foster City, CA, USA). Real-time PCR analysis was performed using the ABI Prism 7500 (Applied Biosystems) by SYBR green chemistry. Primers for PCR analysis are as below: *Actb*, 5′-TGGAATCCTG TGGCATCCATGAAA-3′ and 5′-TAAAACGCAGCTCAGTAACAGTCCG-3′; *Tnfsf13b/Baff*, 5′-AACAGACGCGCTTTCCAG-3′ and 5′-CAGGAGGAGCTGAGAGGTCTAC-3′; *Tnfsf13/April*,

5′-GGTGGTATCTCGGGAAGGAC-3′ and 5′-CCCCTTGATGTAAATGAAAGACA-3′.

Immunofluorescent staining

Acetone-fixed 6-μm thick LN sections were sequentially incubated with primary antibodies and the appropriate fluorescently labeled secondary antibodies after blocking. Sections were mounted with Prolong Gold Anti-fade Reagent (Invitrogen) and examined under IX70 confocal microscope (Olympus, Tokyo, Japan) or BZ-9000 fluorescent microscope (Keyence, Osaka, Japan).

Quantification of medullary remodeling

Images of immunofluorescently stained 6-μm LN sections were obtained and tiled to generate full-section views of each LN section. The medullary region was identified in the tiled images based on the staining pattern of type IV collagen that marks the medullary sinus and differences in stromal networks between the paracortex and the medulla. The pixel number of the total medullary region and Lyve-1$^+$ area therein was counted using the Count Tool of Photoshop CS4 (Adobe Systems, San Jose, CA, USA), and [%Lyve-1$^+$ area in the medulla] was calculated for each LN section (Supplementary Figure S1 is available at *International Immunology* Online). The Lyve-1$^+$ signal was converted to single-bit before quantification. The remodeling index defined as the immunized/non-immunized ratio of [%Lyve-1$^+$ area within the LN medulla]$^{-1}$ was calculated by dividing [%Lyve-1$^+$ area in the medulla]$^{-1}$ on each LN section with the mean value of [%Lyve-1$^+$ area in the medulla]$^{-1}$ on the sections of naive LNs. Naive LNs were taken from mice that were similarly treated and of the same genotype as immunized mice. At least four sections (60–120 μm apart from each other starting from that which represented the largest area of each LN) of a single LN were used to calculate remodeling index of each LN.

Flow cytometry

Single-cell suspensions of LN were sequentially incubated with anti-CD16/32 to block Fc receptors and then primary antibody mixture. For the detection of intracellular NP-binding activity, single-cell suspensions were incubated with NP-PE (Biosearch Technologies) after fixation and permeabilization in Cytofix/cytoperm buffer (BD Bioscience). Data were collected using LSRII (BD Bioscience) or Gallios (Beckman Coulter, Brea, CA, USA) flow cytometers and analyzed using FlowJo software (TreeStar, Ashland, OR, USA).

Adoptive transfer of B cells

Donor B cells were prepared from pooled splenocytes and LN cells of CD45.1$^+$ mice by magnetically depleting CD43$^+$, CD90.2$^+$ and Ter-119$^+$ cells using an autoMACS cell separator (Miltenyi Biotec, Bergisch Gladbach, Germany). The purity of the isolated B cells was >98%. For the homing assay, pre-immunized C57BL/6 recipients were injected intravenously with 5 to 10 × 10^6 purified CD45.1$^+$ B cells, and LNs were isolated from the recipient mice 1 or 16 h after the transfer. For the reconstitution experiment, μMT mice received 2 × 10^7 naive wild-type (WT) B cells (CD45.2$^+$) that were depleted of NP-binding cells 1 day before and after immunization with NP-OVA/CFA. In some experiments, μMT mice received 1 × 10^4 of B1-8 cells at the time of reconstitution with naive WT B cells. B1-8 cells were enriched from pooled splenocytes and LN cells of CD45.1$^+$ IgH^a B1-8 mice by depleting CD43$^+$, CD90.2$^+$, Ter-119$^+$ and Igκ$^+$ cells by autoMACS. The purity of the isolated B1-8-derived B cells (B1-8 cells) was >95%.

ELISA

Titrated serum samples were applied in duplicate onto Maxisorb Immunoplates (Nunc, Roskide, Denmark) pre-coated with NP_{33}-BSA (Biosearch Technologies). Plates were further incubated with HRP-labeled polyclonal anti-mouse IgG1 (Bethyl Laboratories, Montgomery, TX, USA) and were developed with a TMB Substrate Kit (Vector Laboratories).

Preparation of recombinant LTβR-Ig

293H cells (Invitrogen) were transfected with pMKIT-Neo-LTβR-huIgG1, using Lipofectamine 2000 reagent (Invitrogen). Transfectants were selected by neomycin resistance for three passages. Selected transfectants were cultured for 5 days in CD 293 serum-free media (Invitrogen) supplemented with 4 mM L-glutamine and 1 mg ml^{-1} G418. Culture supernatant was harvested, and LTβR-Ig was purified from the culture supernatant by affinity chromatography using a Protein G column.

Statistics

Statistical analyses were performed using GraphPad Prism software. $P < 0.05$ was considered to be statistically significant.

Results

Remodeling of the LN medulla during inflammation

First, we sought to characterize the structural changes that occur in the LN medulla during immune responses. We immunized C57BL/6 mice with NP-OVA emulsified in CFA (NP-OVA/CFA) and analyzed the structure of the LN medulla. On day 8 post-immunization, the medullary region of the DLN displayed enlarged parenchyma and a reduced Lyve-1$^+$ lymphatic sinus area (Fig. 1A). We observed similar changes in BALB/c mice (data not shown). Furthermore, structural change in the LN medulla was also evident upon immunization with NP-OVA adsorbed onto alum adjuvant (NP-OVA/Alum) or upon infection with HSV-1, OVA-expressing vaccinia virus (VV-OVA) or OVA-expressing *L. monocytogenes* (LM-OVA) (Fig. 1B). Subcutaneous immunization with type-1 T-independent antigen CpG oligonucleotide, but not type-2 T-independent antigen NP-Ficoll, induced structural change in the LN medulla. By our protocol, subcutaneous NP-Ficoll immunization induced neither expansion of NP-specific B cells nor DLN hypertrophy (data not shown). These data suggest that structural change in the LN medulla generally occurs during immune responses but possibly requires inflammatory stimuli.

To further characterize the structural changes occurring in the LN medulla, we analyzed the cellular localization and components of the stromal networks therein. We found that stromal re-networking within the DLN medulla was manifested

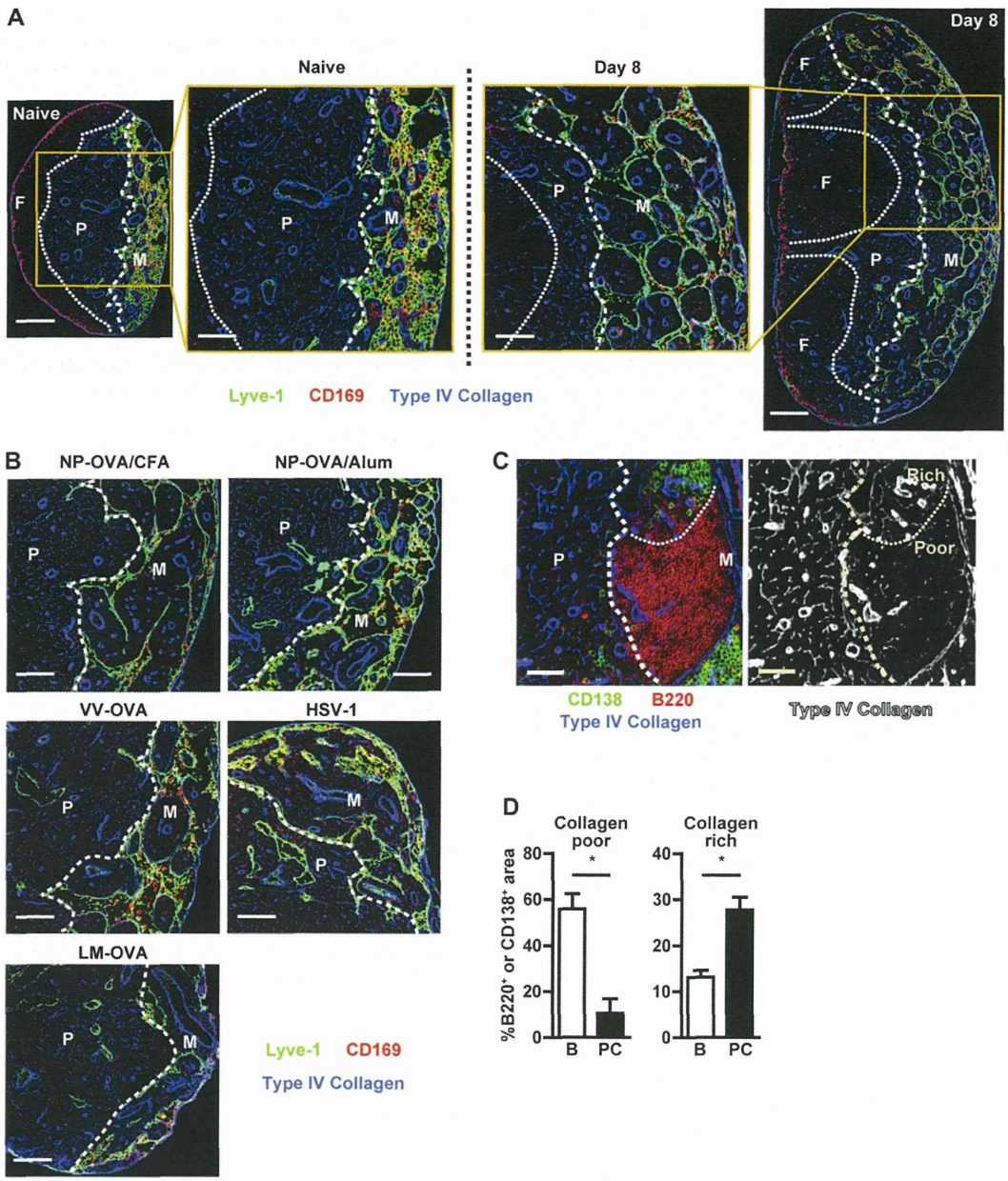

Fig. 1. Remodeling of the LN medulla during immune responses. (A) Immunohistochemistry of the DLN on days 0 (naive, left) and 8 (right) post-immunization with NP-OVA/CFA. Scale bars represent 200 and 100 μm in images of whole LNs (×100) and their inset images (×200), respectively. (B) Medullary remodeling in the DLN of mice immunized with NP-OVA/CFA, NP-OVA/Alum, VV-OVA, HSV-1 or LM-OVA 8 days before analysis. Scale bars represent 100 μm. Original magnification was ×200. (C) Segregation of B cells and plasma cells in the LN medulla on day 6 post-immunization. Collagen-rich and collagen-poor regions are separated by a dotted line and marked Rich and Poor, respectively. Scale bars represent 50 μm. Original magnification was ×200. M, medulla; P, paracortex. (D) Percentage of the $B220^+$ (B, white) and the $CD138^+$ (PC, black) areas in the collagen-poor (left) and collagen-rich (right) regions of the medulla on day 6 post-immunization. Graphs represent the mean and SEM of three mice. $*P < 0.0001$ by Student's (Collagen-poor) or Welch's (Collagen-rich) *t*-test. Representative data from three to five independent experiments ($n = 3$ or 4 for each group per experiment) are shown.

by the appearance of collagen-poor and collagen-rich regions (Fig. 1C). Notably, in the DLN medulla, B cells and plasma cells were predominantly distributed to collagen-poor and collagen-rich regions, respectively (Fig. 1D). Moreover, survival factors for B cells and plasma cells, *Tnfsf13b*/*Baff* and *Tnfsf13*/*April* (33), are expressed in the medulla of inflamed LNs (17), although relative expression of these genes was unchanged between naive and inflamed LNs (Supplementary Figure S2 is available at *International Immunology* Online). Taken together, these data suggest that medullary remodeling of DLNs involves stromal re-networking, which, together with the corresponding survival factors

constitutively expressed in the medulla, may contribute to the accumulation and segregation of B cells and plasma cells within the LN medulla.

Kinetics of medullary remodeling parallels those of changes in plasma cell number in the DLN

To elucidate the relationship between medullary remodeling and the antibody response, we addressed the kinetics of medullary remodeling. For this purpose, we defined a 'remodeling index' as the ratio of [%Lyve-1$^+$ area within the medulla]$^{-1}$ between immunized and naive LNs to quantitatively evaluate the progress of medullary remodeling (see Materials and Methods and Supplementary Figure S1, available at *International Immunology* Online, for details). This index represents the change in the relative size of the medullary parenchyma because the medullary structure is largely composed of lymphatic sinus and parenchyma surrounding blood vessels. By this definition, the remodeling index is equal to 1 in naive LNs and increases as remodeling proceeds. Evaluation of medullary remodeling with this index revealed that the kinetics of remodeling correlate with changes in the number of cognate plasma cells in the DLNs (Fig. 2A and B). After reaching a maximum value between days 6 and 10 post-immunization, the remodeling index declined and returned to a value of 1 at day 21 post-immunization with NP-OVA/CFA. Although the timing of the normalization of remodeling differed between immunization protocols in each case occurring 14–21 days post-immunization, the index value always peaked between days 6–10 post-immunization (data not shown). These data indicate that medullary remodeling during acute inflammation is a transient event that parallels the generation of cognate plasma cells in the DLN.

Cellular conditions required for medullary remodeling

To further characterize the medullary remodeling process, we examined the cellular conditions required for the induction of medullary remodeling. Immune cells, including T cells and DCs, have been reported to be involved in the remodeling of the LN follicles and paracortex (20,22,23). Localization of T cells and DCs to the medulla of inflamed LN, in addition to B cells and plasma cells (data not shown), prompted us to hypothesize that immune cells may also play an important role in medullary remodeling.

First, we examined the potential role of inflammatory monocytes, granulocytes and lymphocytes in medullary remodeling, by using *Ccr2*$^{-/-}$ mice, anti-Ly6G treatment and *Rag2*$^{-/-}$ mice, respectively. Due to the defective egress of inflammatory monocytes from BM, *Ccr2*$^{-/-}$ mice harbor few inflammatory monocytes and the macrophages derived from these monocytes in the periphery (34). Anti-Ly6G treatment depleted >95% of granulocytes. However, the DLNs of *Ccr2*$^{-/-}$ and anti-Ly6G-treated mice subcutaneously immunized with NP-OVA/CFA exhibited medullary remodeling at a comparable level to control mice (data not shown). In contrast, medullary remodeling did not occur in *Rag2*$^{-/-}$ mice (Fig. 3A and B), indicating that lymphocytes play an essential role in this process.

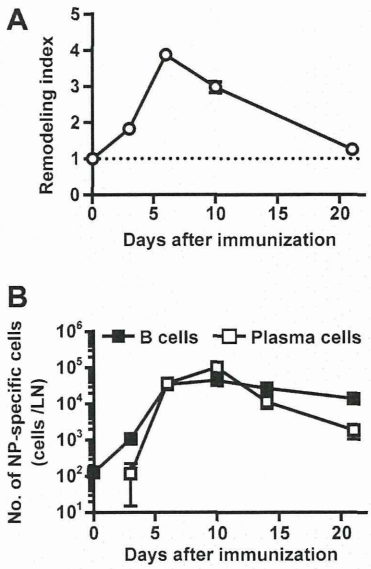

Fig. 2. Kinetic correlation between medullary remodeling and plasma cell generation. (A) Kinetics of medullary remodeling upon immunization with NP-OVA/CFA as measured by the remodeling index (see Materials and Methods and Supplementary Figure S4, available at *International Immunology* Online, for details). The dotted line indicates the index value 1, which represents the medullary condition of a normal LN. (B) Kinetics of the changes in numbers of B220$^+$ B cells (black) and CD138$^+$ plasma cells (white) among NP-binding$^+$ Dump (CD3, CD11b, NK1.1, IgD)$^-$ cells in the DLN of mice immunized with NP-OVA/CFA. NP-specific plasma cells were not detected on day 0. Note the similarity of the curves of plasma cell number and medullary remodeling. Data are expressed as mean ± SEM. Representative data from five independent experiments (n = 3–5 for each group per experiment) are shown.

In order to elucidate the relative contribution of T cells and B cells to medullary remodeling, we analyzed T cell-deficient *nu/nu* mice and B cell-deficient μMT mice. On day 8 post-immunization with NP-OVA/CFA, *nu/nu* mice showed medullary remodeling at a comparable level to WT mice (Fig. 3C and D), indicating that T cells make little contribution to this process. In contrast, similarly treated μMT mice failed to display medullary remodeling (Fig. 3E and F). Furthermore, adoptive transfer of 2×10^7 polyclonal naive B cells into μMT mice 1 day before and after immunization restored medullary remodeling, confirming the essential role of B cells in this process (Fig. 3G and H).

T-dependent B-cell response is not an absolute requirement for medullary remodeling

Due to the lack of T cells, *nu/nu* mice failed to mount T-dependent B-cell responses (data not shown), suggesting that expansion of cognate B cells during the response may not be a prerequisite for the induction of medullary remodeling. In order to confirm this in WT mice, we employed antibody-mediated depletion of CD4$^+$ T cells.

WT mice were treated with anti-CD4 depletion antibody on days −3 and −1, immunized with NP-OVA/CFA on day 0 and analyzed on day 8. Under this protocol, anti-CD4 antibody treatment achieved >98% depletion of CD4$^+$ T cells

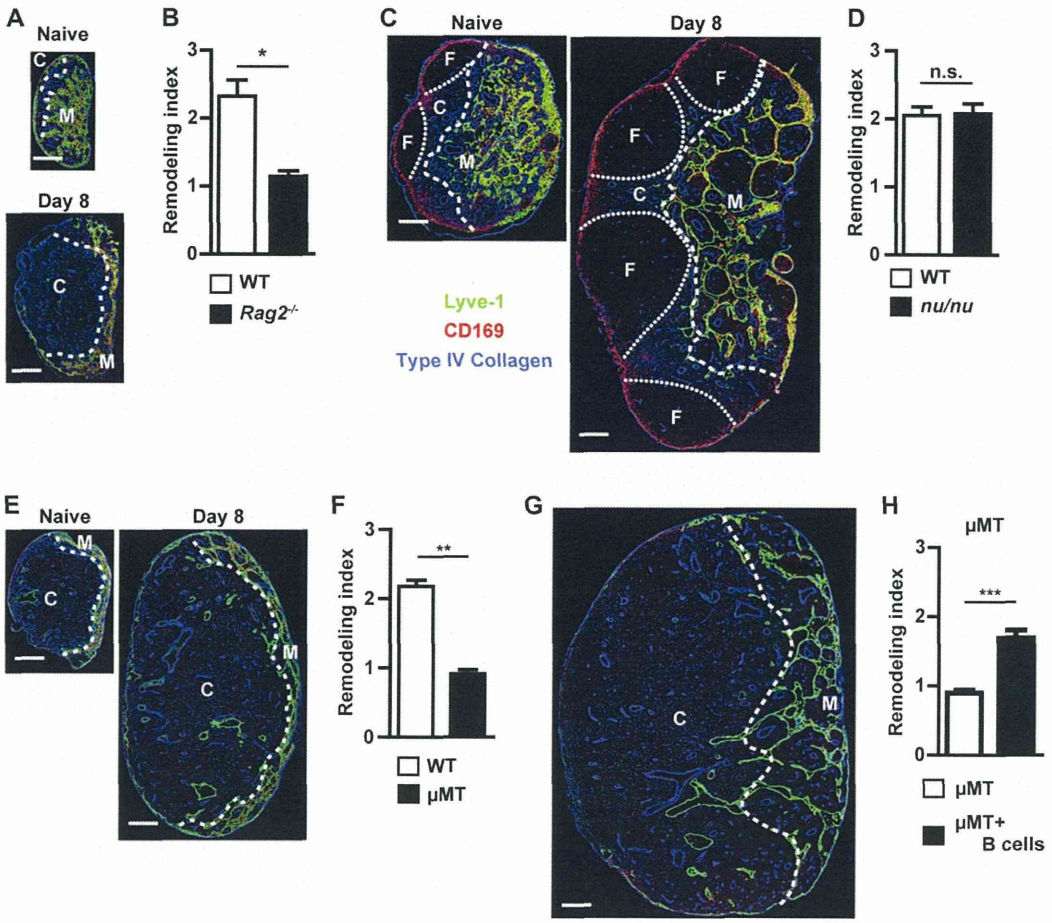

Fig. 3. Cellular conditions required for medullary remodeling. Immunohistochemistry and the remodeling index of the DLN of *Rag2*$^{-/-}$ (A and B), *nu/nu* (C and D) and μMT (E and F) mice immunized with NP-OVA/CFA. (A, C, E and G) Immunohistochemistry of the DLN on days 0 (naive) and 8 post-immunization. Scale bars represent 200 μm. Original magnification was ×100. C, cortex; M, medulla and F, follicle. (B, D, F and H) Remodeling index of WT (white) and mutant (black) mice on day 8. (G and H) μMT mice were injected with 2×10^7 WT B cells 1 day before and after immunization. Control mice did not receive B cells. Graphs show mean and SEM. $^*P < 0.01$, $^{**}P < 0.0005$, $^{***}P < 0.0001$, n.s., not statistically significant by Student's *t*-test. Representative data from three independent experiments ($n = 3$–5 for each group per experiment) are shown.

(data not shown). As expected, CD4$^+$ T cell-depleted WT mice mounted only a minimal anti-NP B-cell response (Fig. 4A). However, the medullary remodeling process remained intact in these mice (Fig. 4B and C), demonstrating that clonal expansion of cognate B cells is not an absolute requirement for medullary remodeling to occur. These results indicate that non-cognate B cells can contribute to remodeling of the LN medulla.

Signaling through LTβR contributes to medullary remodeling

Our results demonstrate that B cells are the essential cell subset in medullary remodeling. However, it remains unclear what molecule(s) are responsible for the induction of medullary remodeling. Considering its essential role not only in the development and maintenance of lymphoid tissues but also in the LN remodeling (35,36), one hypothesis is that lymphotoxin-α1β2 signal is provided by B cells (and probably other immune cells as well) to medullary stromal cells through LTβR. We therefore tested whether blocking LTβR ligands by recombinant LTβR-Ig affects medullary remodeling.

Mice were injected with LTβR-Ig 1 day before and after immunization with NP-OVA/CFA. We found that LTβR-Ig, but not control Ig, partially inhibited medullary remodeling (Fig. 5A and B; 55% reduction in remodeling index value relative to control). However, this result should be interpreted carefully because LTβR-Ig treatment is also known to abrogate high endothelial venule (HEV) function (37) as well as depleting FDCs (38), both of which could affect medullary remodeling by modifying B-cell activation. In fact, the number of NP-specific B cells in NP-OVA/CFA-immunized mice treated with LTβR-Ig was reduced to ~37% of the cell number in control mice, although the difference was not statistically significant. Despite a reduced number of NP-specific B cells, FDC-deficient *Cxcr5*$^{-/-}$ BM chimeric mice displayed medullary remodeling to a comparable extent as their WT counterparts (Supplementary Figure S3 is available at *International Immunology* Online), indicating that loss of FDCs

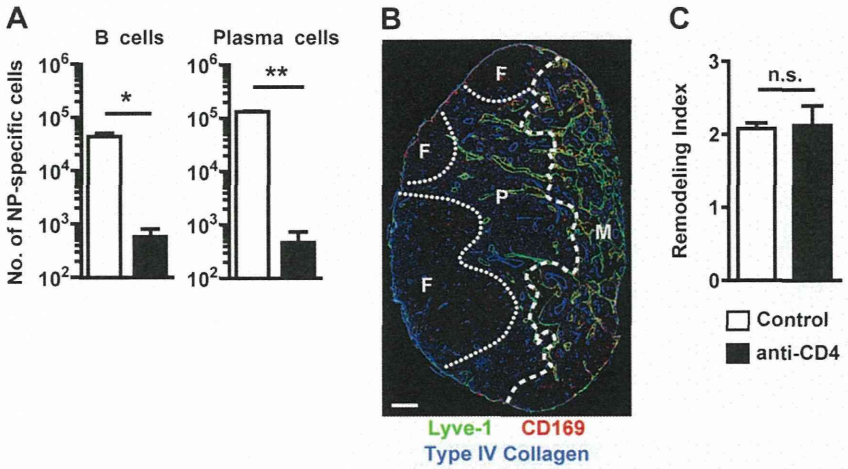

Fig. 4. Contributions of non-cognate B cells to medullary remodeling. C57BL/6J mice were treated with anti-CD4 or control Ig on days −3 and −1, immunized with NP-OVA/CFA on day 0 and analyzed on day 8. (A) The number of $B220^+$ B cells and $CD138^+$ plasma cells among NP-binding$^+$ Dump$^-$ cells. (B) Immunohistochemistry of the DLN from anti-CD4-treated mice. (C) Remodeling index of the DLN from control Ig-treated (white) and anti-CD4-treated (black) mice. $*P < 0.05$, $**P < 0.01$ by Welch's *t*-test; n.s., not significant by Student's *t*-test. Representative data from three independent experiments ($n = 4$ or 5 for each group per experiment) are shown.

and the resulting curtailed B-cell response has minimal effect on medullary remodeling. Of note, although plasma cell number was also reduced, their localization to the medulla was unaffected (Fig. 5C and D). In these mice, B cell entry into the DLN was also moderately decreased on day 7 post-immunization but remained unaffected prior to this (Fig. 5E). Accordingly, it is unlikely that this effect is responsible for the inhibition of the remodeling process, considering the kinetics of medullary remodeling (Fig. 2B). Although the exact cellular target of LTβR-Ig remains unclear, these results suggest that signaling through LTβR contributes to medullary remodeling in a manner that is independent of FDC networks and HEV homeostasis.

Reconstitution of μMT mice with non-cognate B cells restores the antibody response by BCR-knock-in B cells

In order to elucidate the functional role of medullary remodeling in humoral immune responses, we performed B-cell reconstitution in μMT mice in combination with adoptive transfer of 1×10^4 $CD45.1^+$ IgH^a NP-specific BCR-knock-in B cells (B1-8 cells). We then immunized mice with NP-OVA/CFA and analyzed how the restoration of medullary remodeling affects humoral immune response by B1-8 cells (Fig. 6A). Under these experimental conditions, WT and B cell-reconstituted μMT (μMT(+)) mice, but not non-reconstituted μMT (μMT(−)) mice, displayed medullary remodeling (Fig. 6B). The remodeling index value was comparable between μMT(+) and WT recipients, although the number of B1-8 B cells in μMT(+) mice was ~15% of that in WT mice. In contrast, the number of B1-8 plasma cells and the serum titer of B1-8-derived anti-NP $IgG1^a$ were comparable between μMT(+) and WT mice, whereas B1-8 cells in μMT(−) mice mounted only a minimal anti-NP response (Fig. 6C and D). Notably, there were no significant differences in the key components of the humoral immune response between μMT(+) and μMT(−) mice such as in the FDC network or the number of follicular helper T cells and subcapsular macrophages (Supplementary Figure S4 is available at *International Immunology* Online). Thus, the restoration of expansion of B1-8 cells in μMT(+) mice was not due to a difference in these components. These results suggest that medullary remodeling has a significant effect on the expansion of plasma cell number in DLNs.

Discussion

In the present study, we demonstrated that B cells and signaling via LTβR play an essential role in the induction of medullary remodeling during inflammation, although the cellular source and target of lymphotoxin signaling remains to be identified. We also found that medullary remodeling occurred even in the absence of T cells, monocytes and granulocytes. Importantly, our results showed that medullary remodeling contributed to the antibody response.

Given that myeloid cells is partly responsible for creating the cytokine milieu in the medulla (17), it is conceivable that B cells and myeloid cells play different, if not independent, roles in the conditioning of the medullary plasma cell niche through the regulation of medullary structure and cytokine milieu, respectively. An important finding of the present study is the antigen specificity of the lymphocytes contributing to LN remodeling. The antigen specificity of such lymphocytes has remained elusive, despite a well-documented role for lymphocytes in LN remodeling (20,22,24). We found that antigenic stimulation of B cells is not a prerequisite for medullary remodeling, although it is likely that cognate B cells relocating to the medulla from the follicles also contribute to this process. Thus, our results define a new role for non-cognate B cells in the humoral immune response as a regulatory component of LN structure, which potentially affects the medullary plasma cell niche. This is in addition

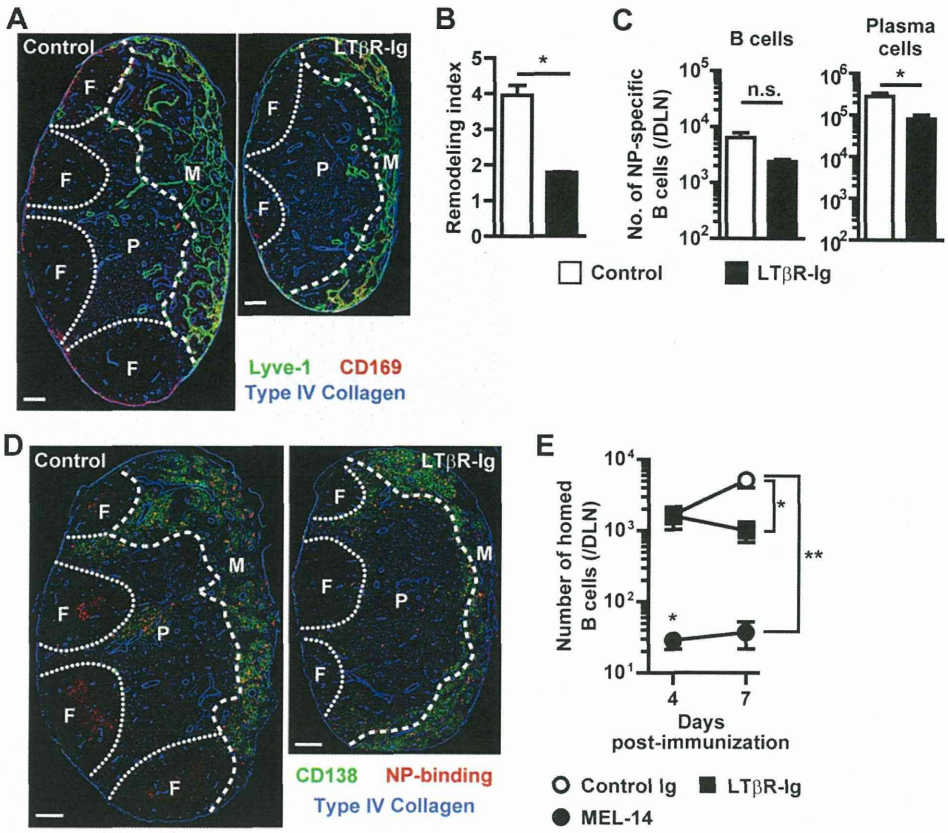

Fig. 5. Involvement of LTβR signaling in medullary remodeling. WT mice were treated with control-Ig or LTβR-Ig on days −1 and 1, immunized with NP-OVA/CFA on day 0 and analyzed on day 8. (A) Immunohistochemistry of the DLNs from mice treated with control-Ig (left) or LTβR-Ig (right). (B) Remodeling index of the DLN of control-Ig-treated (white) and LTβR-Ig (black)-treated mice. (C) The number of $B220^+$ B cells and $CD138^+$ plasma cells among NP-binding$^+$ $Dump^-$ cells in the DLN of control-Ig- or LTβR-Ig-treated mice were measured by flow cytometry. (D) Localization of plasma cells in the DLN on day 8. Note that $CD138^+$ cells were mostly localized in the medulla in both groups. (E) Homing of naive B cells to DLN. $CD45.1^+$ naive polyclonal B cells were transferred 1 h before sacrifice at the indicated time points. The number of $CD45.1^+$ $B220^+$ cells in the DLNs. Results from MEL-14-treated mice are shown as a positive control for the inhibition of B cell homing to LN. Statistical differences were evaluated between control and MEL-14- or LTβR-Ig-treated mice. On day 4, there was no significant difference between control and LTβR-Ig-treated mice. Scale bars represent 200 μm. Original magnification was ×100. $^*P < 0.05$, $^{**}P < 0.01$, n.s., not significant by Welch's *t*-test (B and C) or one-way analysis of variance with Dunnett's *post-hoc* (E). Graphs show mean and SEM. Representative data from three independent experiments ($n = 4$ or 5 for each group per experiment) are shown.

to the recently reported role of these B cells in complement receptor 2 (CR2)-dependent immune complex relay into the germinal center (9).

In our reconstitution experiment using μMT mice, restoration of medullary remodeling resulted in the recovery of the number of plasma cells derived from adoptively transferred B1-8 cells. Our data show that this is unlikely to be due to differences in the number of FDCs and follicular helper T cells, which play important roles in antigen presentation and B-cell differentiation (21,39). CR2-dependent immune complex relay is also unlikely to be responsible because *Cr2* deficiency in hematopoietic cells is reported not to affect the B-cell response at least until day 7 post-immunization (9). In addition to a quantitative correlation, we also observed a kinetic correlation between antigen-specific plasma cell number in the DLN and the extent of medullary remodeling, reinforcing contribution of this process to the antibody response. Of note, although plasma cell number was greatly reduced in the absence of medullary remodeling, the remaining plasma cells were localized to the medulla independently of medullary remodeling. This finding suggests that the LN medulla is intrinsically capable of holding plasma cells to some extent but that medullary remodeling is required to support a maximal response. Consistent with this idea, expression of *Baff* and *April* was constitutively detected in the medulla, which raises a possibility that per-cell availability of BAFF and APRIL in the medulla remains unchanged during medullary remodeling. Thus, our findings suggest that the LN medulla is actively restructured in such a way that it expands to accommodate, rather than newly create, the medullary plasma cell niche in DLNs.

Recently, Kumar *et al.* reported the critical role of B cells and lymphotoxin-β in the elongation and branching of HEV in the DLN, which lead to LN expansion during lymphocytic choriomeningitis virus infection (24). Their 3D imaging analysis also revealed that B-cell volume is increased in the DLN

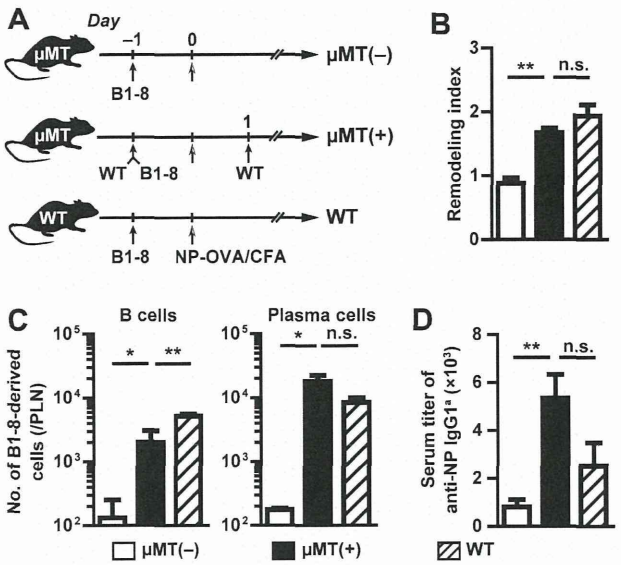

Fig. 6. B-cell reconstitution in μMT mice restores the expansion of adoptively transferred B1-8 cells. (A) Experimental protocol. μMT mice were reconstituted with two injections of 2×10^7 WT B cells. Together with the first injection of WT B cells, 1×10^4 CD45.1$^+$ IgH^a B1-8 cells were transferred. As a control for B cell-sufficient condition, WT mice were similarly treated except did not receive B-cell transfer. The structure of the DLN, the number of CD45.1$^+$ B1-8 B cells (B220$^+$) and plasma cells (CD138$^+$) and the serum titer of anti-NP antibody derived from B1-8 cells were analyzed on day 8. (B) Remodeling index of the DLN. (C) The number of B1-8 B cells and plasma cells in the DLN. (D) Serum titer of anti-NP IgG1^a. $^*P < 0.05$, $^{**}P < 0.01$, n.s., not significant by one-way analysis of variance with Dunnett's *post-hoc*. Representative data from two independent experiments ($n = 3$–5 *for each group per experiment*) are shown.

during the infection. Although the position of B-cell clusters (i.e. the follicles or medulla) was not specified in this report, *accumulation of B cells in the medulla during inflammation* and medullary remodeling suggests that increased B-cell volume in the DLN is the net result of follicular expansion and medullary remodeling. Importantly, our results added a new insight into the function of B cell-mediated LN remodeling as a process that regulates antigen-specific antibody response in LNs.

Kataru *et al.* recently documented that T cells and B cells counterbalance each other to regulate the growth of LN lymphatic vessels (40). In agreement with their observations in whole LN sections, we confirmed that lymphatic vessel density was also larger in the LN medullary region of naive *Rag2*$^{-/-}$ and *nu/nu* mice than in WT and μMT mice (data not shown). This observation could potentially have affected our results in a manner that decreases the remodeling index value in T cell-deficient mice due to an increased [%Lyve-1$^+$ area in the medulla]$^{-1}$ of naive LN. However, by our definition of the remodeling index as the immunized/naive ratio of [%Lyve-1$^+$ area in the medulla]$^{-1}$, the index represents the fold-change in medullary parenchyma to lymphatic sinus ratio. Based on our results, we conclude that the fold-change in the medullary parenchymal area from steady to inflammatory state is not affected by the loss of T cells.

As described above, loss of lymphocytes substantially *affects the homeostasis of LN structure. However, comparable* %Lyve-1$^+$ values between WT and μMT mice may suggest that B cells play only a marginal role in homeostatic development and maintenance of medullary structure but are essential for its remodeling during inflammation. In addition, abrogated lymphotoxin signaling may also alter the homeostatic maintenance of medullary structure. In fact, LTβR-Ig treatment decreased %Lyve-1$^+$ within LN medulla in unimmunized mice, suggesting that lymphotoxin signaling is involved in the homeostatic maintenance of LN lymphatic vessels. Although it seems likely that lymphotoxin signaling affects the homeostasis of the LN medullary stroma, this hypothesis remains to be confirmed by further experimentation.

In another report by Angeli *et al.* (22), it was demonstrated that B cells are also implicated in LN lymphangiogenesis through vascular endothelial growth factor (VEGF) production, which facilitates DC migration to LNs. Since LTβR-Ig only partially inhibited medullary remodeling, VEGF may also play a role in medullary remodeling as an additional molecular component. One inconsistency with the previous study is that Angeli *et al.* reported an increased %Lyve-1$^+$ area in DLNs (region not specified), whereas we observed a decreased %Lyve-1$^+$ area in the inflamed LN medulla. This difference in results may have arisen due to the foci of the report from Angeli *et al.*, which analyzed lymphangiogenesis in terms of the portal of entry for DCs. However, we do not consider lymphangiogenesis in the paracortex and medullary remodeling to be mutually exclusive.

Lymphocytes play a critical role in the maintenance of the dynamic equilibrium of LN size and structure (35,36,41). The independence of medullary remodeling from the T-dependent B-cell response encourages us to speculate that inflammatory stimuli, especially Toll-like receptor ligands, may upset this equilibrium, triggering the remodeling process. In support of this idea, B cells stimulated with Toll-like receptor ligands or anti-CD40 up-regulate surface lymphotoxin-β expression (42,43). *This phenomenon could be responsible for* conferring non-cognate B cells with the ability to contribute to medullary remodeling, considering that CpG-oligonucleotide, but not NP-Ficoll, induces medullary remodeling. Moreover, Toll-like receptor ligands have been reported to act on vascular endothelial cells in LNs, promoting vascular re-organization and in turn lymphocyte recruitment to DLNs (25), which leads to accumulation of B cells. Another area for investigation is the effect of inflammatory stimuli on medullary stromal cells and the possible resulting changes in B-cell retention. We speculate that inflammatory stimulation of lymphocytes, stromal cells and endothelial cells in LNs triggers a positive feedback loop between B-cell accumulation and the expansion of the medullary niche for plasma cells. Medullary remodeling would be initiated by the first cohort of B cells recruited to the LN medulla that are likely to consist mostly of non-cognate cells. Once initiated, medullary remodeling expands the niche available for the subsequent arrival of additional cohorts of activated B cells and plasma cells. In addition, relocation of activated cognate B cells from the follicles to the medulla and the promotion of medullary remodeling by these B cells may constitute another feedback loop. These putative feedback loops may